IEEE Photonics Journal
An IEEE Photonics Society Publication

Open Access

Flexible 16 × 10-Gb/s All-Optical Broadcast and Multicast TWDM Passive Optical Network

Volume 7, Number 4, August 2015

M. S. Salleh
A. S. M. Supa'at
S. M. Idrus
Z. M. Yusof
S. Yaakob

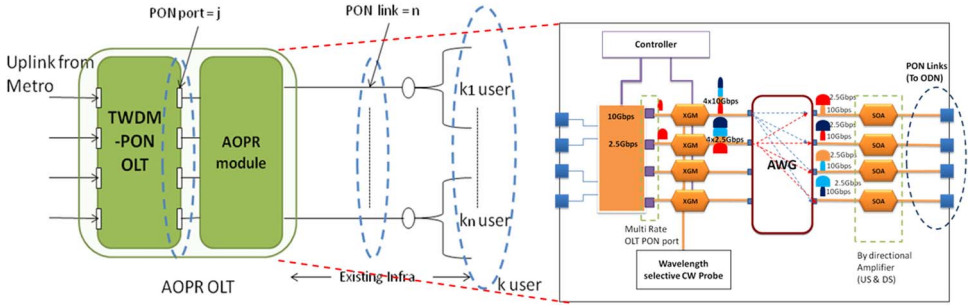

DOI: 10.1109/JPHOT.2015.2456058
1943-0655 © 2015 IEEE

IEEE photonics SOCIETY

IEEE

Flexible 16 × 10-Gb/s All-Optical Broadcast and Multicast TWDM Passive Optical Network

M. S. Salleh,[1,2] A. S. M. Supa'at,[2] S. M. Idrus,[2] Z. M. Yusof,[1] and S. Yaakob[1]

[1]Photonic, Communication Technologies, TMR&D Sdn Bhd, Cyberjaya 63000, Malaysia
[2]Universiti Teknologi Malaysia, Johor Bahru 81310, Malaysia

DOI: 10.1109/JPHOT.2015.2456058

Manuscript received March 28, 2015; revised July 3, 2015; accepted July 8, 2015. Date of publication July 13, 2015; date of current version August 18, 2015. Corresponding author: M. S. Salleh (e-mail: shah@tmrnd.com.my).

Abstract: To achieve flexible packet routing in a time wavelength-division multiplexing passive optical network (PON) architecture, most proposed systems use a tunable transceiver in the optical line terminal (OLT). The tunable transceiver is attractive for use in a PON system because it is able to broadcast and multicast packets within the entire PON system, being limited only to a single PON link. The proposed all-optical packet routing (AOPR) module was designed to incorporate a fixed-type wavelength OLT transmitter with a continuous-wave pump probe signal module. The design of the module is based on the ALL-ON method to support all broadcast signals, which replaces the wavelength tuning feature in the tunable OLT transmitter. The proposed architecture was designed using the multicasting cross-gain modulation (XGM) method. In this proposed design, the XGM function of the OLT system becomes a part of the AOPR OLT transmitter. The arrangement of this design aims to generate single or multiple wavelengths in a downstream direction in each OLT PON port. The measurement results revealed that the proposed system can handle a total of 160-Gb/s broadcast downstream bandwidth to serve 16 PON links using 16λ with a maximum of 2048 users.

Index Terms: TWDM PON, all-optical packet routing, semiconductor optical amplifier, cross gain modulation, broadcasting and multicasting packet, NG-PON2.

1. Introduction

Many approaches have been used to support high numbers of users and long-reach systems [1]–[3] in a TWDM PON system. One of these approaches is to design a single TWDM PON system with multiple PON ports to manage multiple PON link interconnects [4]–[6]. This architecture was designed to extend the TWDM PON system proposed by ITU-T in next-generation PON 2 (NG-PON2) system requirements [7]. However, this architecture has the following issues: 1) reduced flexibility of the system to handle the full function of broadcasting or multicasting while simultaneously handling the multiplexing of multiple wavelengths with different PON ports at different PON links within a single TWDM PON system; 2) high cost of fiber deployment to support an existing ODN and fiber infrastructure; and 3) complex design of the system to handle multiple access technologies, such as GPON, XG-PON, and TWDM PON, at different PONs. In designing a flexible TWDM PON system, most of the proposed architectures use a tunable wavelength laser source (TWLS) [8], [9] or multiple fixed multi-wavelength (FMW) [6]

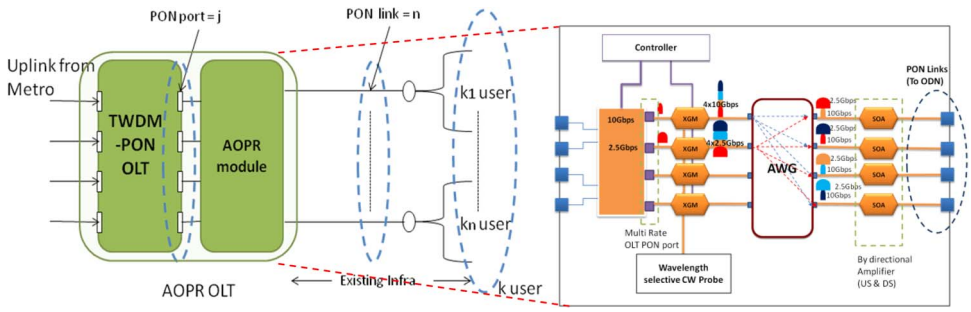

Fig. 1. Proposed AOPR WDM/TDM PON system architecture.

transmitters in an OLT PON port; such sources enable flexible wavelength routing (WR) and multiplexing of the signal in the downstream signal. However, tunable laser source (TLS) signals have limitations in providing full broadcast or multicast within an entire TWDM PON system because the TLS will transmit only a single wavelength and this signal will be routed only to a single PON link. Another challenge for a TLS involves re-routing a certain packet at a different PON link because TLS requires time to tune the wavelength [10], [11], which will cause a wavelength tuning delay in the system, thereby affecting performance. The use of a multi-channel wavelength transmitter also faces issues because high numbers of OLT transmitters connected to a single PON port will incur an additional cost to the system. In addition, the use of many different types of transmitters will introduce inventory issues and will increase the possibility of human error during system installation or maintenance.

2. AOPR TWDM PON System Architecture

Few studies have described a flexible design in a TWDM PON system [4], [12]–[16]. Kani and Dixit described in detail a type of flexible architecture design of a TWDM PON system based on certain criteria and requirements. The present study proposed a novel architecture for an AOPR TWDM PON system. The proposed system allows distributing each output of several (or all) OLT ports to all the PON links without using the plenty of multi wavelength laser. A generic AOPR TWDM PON system architecture design is shown in Fig. 1, and the downstream schematic of the proposed architecture can be found in right side illustration of Fig. 1. The module comprises components such as multiple ports of OLT, wavelength converter or XGM module using SOA, multi-channel CW laser, N × N AWG, fiber delay line, optical coupler, and electronic controller. The general description of each component is as follows:

- Multiple OLT PON port: This port (e.g., 4 or 8) is controlled by a single PON controller. This function enables PON controller to control routing and switching packet between uplink layer from/to the metro network to PON network. This allows PON controller to control flexible bandwidth managements in each OLT PON port.
- XGM module: It comprises SOA. This module is specifically designed to convert original wavelength into new wavelength according to cyclic AWG input and output port.
- CW PPS module: It comprises multiple CW lasers with different wavelengths. This module is designed to support wavelength conversion using XGM module. Two methods of probe signal are used in this system: first, ON and OFF signal to support packet routing and multicast signal, and second, ON signal to support full broadcasting function.
- N × N AWG: This is an interconnecting medium between multiple PON OLT ports and multiple PON ODN links. In this module, AWG is used as a wavelength filter to avoid unwanted WR to undefined OLT or PON ODN link. Another function of AWG is to filter ASE signal generated from SOA.
- Bidirectional amplifier: Both upstream and downstream signals need to be amplified to support more split numbers and longer distances. In this module, SOA is used in both directions.

- Controller: A processor (or controller) controls the multiple OLT PON ports and other components in the module.

Under the same existing fiber plant (same ODN and fiber network), the proposed system introduces new elements in the OLT module to support all-optical routing functions. This function enables each PON port to route its packet to any PON destination link, N. In this design, each PON port, j, could handle up to $\sum[i = 1, n]k(i)$ customers using the single PON port. The downstream signal from each PON link transmits a broadcast packet to k customers at different wavelengths in broadcast mode according to its packet destination ID. This proposed system is composed of an OLT module, an ODN module and ONU modules. The OLT module located in the CO contains multiple OLT PON ports that are integrated with the newly proposed AOPR module design. The module is composed multiple OLT ports, a wavelength converter or XGM module using SOA, a multi-channel continuous wave (CW) laser, an N × N AWG, an optical coupler, and an electronic controller. This module provides connections between multiple OLT PON ports and multiple PON ODN links. This design enables the system to extend communication to support more users in a single TWDM PON OLT system. To support the coexistence network design, this system architecture was designed to use the existing ODN infrastructure that is currently used by legacy GPON and XG-PON systems through an optical splitter to broadcast the downstream signal. The ONU module used to support the TWDM PON system must be able to support wavelength filtering to filter the GPON and XG-PON downstream wavelengths.

The combination of an SOA and an AWG will grant full flexibility of the PON system to operate as an AOPR in the physical layer, thereby reducing the routing and aggregation function requirements in the uplink PON system. In the proposed design, to support the XGM function, the nonlinearity region is a critical point for both input signals injected as an input to the SOA. The SOA must have the capability to accept low input power from the OLT PON port and CW PPS. At the saturation region, XGM will pattern the continuous wave (CW) signal to follow the original "high and low" or "1 and 0" ON and OFF signal according to the OLT downstream data. The XGM principle is based on the gain variation of the SOA after it reaches the saturation point. In the SOA, gain saturation, G_{sat} and $G_{\text{sat\_multi}}$ is defined as follows [17]:

$$G_{\text{sat}} = \frac{G_O}{1 + \frac{P_{\text{probe}} + P_{\text{pump}}}{P_{\text{sat}}}} \quad \text{or} \quad G_{\text{sat\_multi}} = \frac{G_O}{1 + \frac{\sum_{i=1}^{n} P_{\text{probe}} + P_{\text{pump}}}{P_{\text{sat}}}} \tag{1}$$

where g_o is the unsaturated material gain; I is the input intensity, which can be calculated as $P_{\text{probe}} + P_{\text{pump}}$; and P_{sat} is the saturation intensity. At the saturation region of the SOA, the gain of the probe signal varies inversely with the input power of the input signal. Thus, the data of the input signal are then inversely transferred to the probe signal [18]. Gain saturation $G_{\text{sat\_multi}}$ is defined to support broadcasting or multicasting XGM, where $\sum_{i=1}^{N} P_{\text{probe}}$ is the total power of n broadcasting or multicasting CW signals in the CW PPS module.

3. AOPR TWDM PON System Modeling and Design Parameter

The system model of the AOPR TWDM PON is shown in Fig. 2. Two optical signals are injected at the input of the SOA and are combined by an optical splitter. The pump signal or OLT downstream signal carrying the modulated signal is described using an optical power P_{pump} centered at λ_s. The CW PPS signal is the probe signal centered at λ_T carrying a CW signal. The number of CW PPS signals depends on the method of the AOPR TWDM PON system, that is, whether the system is used to support flexible multicast routing (i.e., multiple signal CW lasers will be ON) or uses All ON to transmit all of the multiple CW PPS signals. SOA1 acts as a wavelength converter based on the XGM process, which is described using a spontaneous emission factor $(\beta_{\text{SOA\_total}})$, effective Gain Go, and an SOA saturation power Psat. The AWG will act as an optical band pass filter at the XGM module output to filter the original OLT data $(P_{\text{pump}}, \lambda_s)$ and route the CW probe signal $(P_{\text{probe}}, \lambda_T)$ to the desired AWG output port.

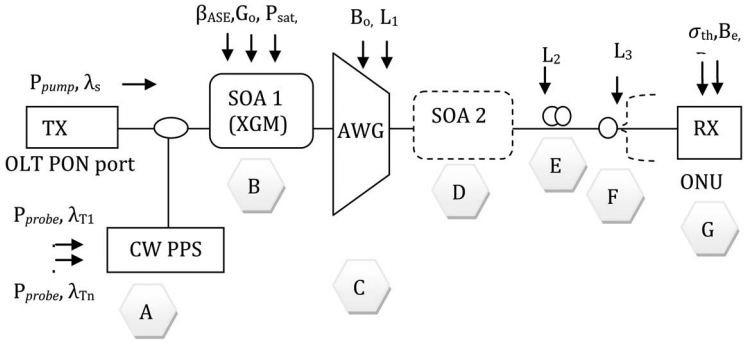

Fig. 2. AOPR TWDM PON system.

In addition to introducing additional loss, the AWG will also introduce additional crosstalk (for example, out-of-band or in-band crosstalk). The system performance degrades whenever crosstalk leads to the transfer of power from one channel to another [19]. The optical signal is received after a link loss L, which occurs due to fiber loss (assumed as the fixed loss rate per km with a typical value of 0.25 dB/km) and the optical splitter (based on the number of split ratios and expressed as L_2 and L_3). The optical receiver is described using an electrical bandwidth B_e, which is correlated with the system operating bandwidth. The receiver is also described using the input-received sensitivity (P_{sens}). Signal degradation in a wavelength conversion-based SOA is caused by Gaussian and non-Gaussian distributed noise. Gaussian distributed noise is primarily due to the amplified spontaneous emission (ASE) at the output wavelength converter, shot noise, and thermal noise at the receiver end. Non-Gaussian distributed noise is primarily due to converted signal noise [20].

A simple calculation of the BER is obtained by adding the equivalent variances of the Gaussian and non-Gaussian distributed noise at the receiver as follows [17]:

$$S(1) = \left[G\left(P^1_{\text{pump}}\right) \cdot r \cdot L \cdot P_{\text{probe}} \cdot \frac{q}{hv}\right]^2 \tag{2}$$

$$S(0) = \left[G\frac{\left(P^0_{\text{pump}}\right)}{r} \cdot L \cdot P_{\text{probe}} \cdot \frac{q}{hv}\right]^2 \tag{3}$$

where q is the electron charge, and $G \cdot (P^0_{\text{pump}})$ and $G \cdot (P^1_{\text{pump}})$ are the gain when the zero and on signal levels, respectively, are injected at the input XGM module. The relationship between $G \cdot (P^0_{\text{pump}})$ and $G \cdot (P^1_{\text{pump}})$ to the output extinction ratio of the XGM module r_{out} is given in [23]

$$r_{\text{out}} = \frac{G\left(P^0_{\text{pump}}\right)}{G\left(P^1_{\text{pump}}\right)}. \tag{4}$$

The noise ratio can be measured by adding both mark and space noise for all of the noise received by the photo detector at the ONU receiver.

Two main design parameters will be measured in this study during the simulation and experimental arrangement. The first parameter is the ONU received sensitivity (P_{sen}). The second parameter is the total link loss budget $(\text{Total}_{\text{LLb}})$. In a PON system, the total allowable link loss budget will determine the numbers of split ratios and the maximum distance of the system from OLT to ONU. The downstream loss budget in an AOPR TWDM PON system is measured from the AOPR OLT output port to the ONU received port. The downstream signal was detected using the ONU, and the BER was evaluated using the error detector.

- *Bit error rate/Bit error ratio (BER)*: In this study, the system assumes the use of a FEC [21], [22] capable of accommodating a BER below 10^{-3}. BER can be calculated on the basis of

the sources of errors: bit 1 at the probabilities of receiving a 1 bit, $P(1)$, and bit 0 at the probabilities of receiving a 0 bit, $P(0)$, which can be included through the error probability, as defined in the equation proposed by Agrawal [19]

$$\text{BER} = P(1)P\left(\frac{0}{1}\right) + P(0)P\left(\frac{1}{0}\right) \tag{5}$$

where $P(0/1)$ is the probability of deciding 0 when a 1 bit is received and $P(1/0)$ is the probability of deciding 1 when a 0 bit is received. The following equations (6 to 8) show the relationship between BER and the Q factor [17], [23]:

$$\text{BER} = \frac{1}{\sqrt{\pi}} \cdot \frac{\exp\left(-\frac{Q^2}{2}\right)}{Q} \tag{6}$$

$$Q = \sqrt{\frac{\text{SNR}}{4}} \tag{7}$$

$$\text{SNR (dB)} = 20\log\left(\frac{\sqrt{S(1)} - \sqrt{S(0)}}{\sqrt{\beta_{\text{total}}(1)} + \sqrt{\beta_{\text{total}}(0)}}\right). \tag{8}$$

- *The minimum average launch power* (P_{tr}): The average launch power P_{tr} is generally known for any transmitter. The power budget is measured in dB and can be expressed in dBm. The minimum average power required by the receiver can be expressed as

$$P_{\text{tr}} = P_{\text{sen}} + C_L + M_s + W_P \tag{9}$$

where C_L is the total loss, M_s is the system margin, and W_P is the loss in the AOPR TWDM PON due to different wavelength penalties (power margins) at different AOPR OLT output ports. C_L in the PON system considers all possible sources of power loss and can be written as

$$C_L = \alpha_f L + \alpha_{\text{con}} + \alpha_{\text{splice}} + \alpha_{\text{split}} \tag{10}$$

where α_f is the fiber loss in dB per kilometer, α_{con} and α_{splice} account for the connector and splice losses and $\alpha_{\text{total\_split}}$ accounts for the optical splitter loss in dB, which depends on the number of splittings in the PON network and can be calculated as

$$\alpha_{\text{split}} = 3(y) + 0.5 \tag{11}$$

where y is the number of stages in a multistage splitter; assuming a $k = 2^y$ way splitter and y is 3, the splitter is a 1×8 splitter $(k = 8)$.

- *PON system reach* $(\text{PON}_{\text{reach}})$: The reach or distance of the PON system is measured between the OLT and the farthest ONU in the system. In the PON system, the reach is related to the number of splittings in the PON system. Based on the link loss budget, the system can be used to estimate the maximum reach of the ONU from the OLT as

$$\text{PON}_{\text{reach}} = \frac{\text{Total}_{\text{LLB}} - (\alpha_{\text{con}} + \alpha_{\text{splice}} + \alpha_{\text{split}} + M_s + W_P)}{\alpha_f} \tag{12}$$

where W_p is the different wavelength power penalty margin due to the different wavelengths and the AWG loss at different PON links.

- *Total Users per PON Link* $(T\_\text{user}_{\text{PON link}})$: In the AOPR TWDM PON system, the maximum number of users per PON link j is determined using the number of split ratios k and the maximum number of cascading splitters within a single PON link. This ratio is related to the

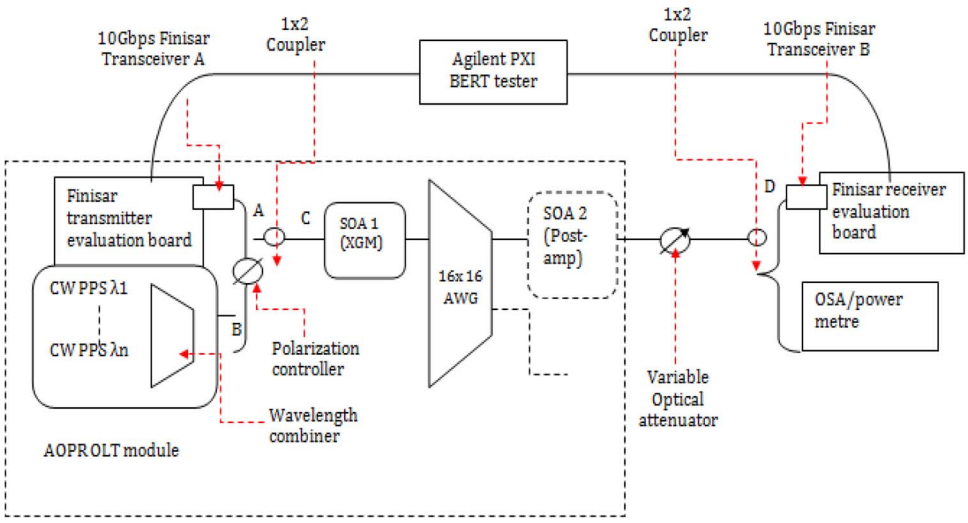

Fig. 3. Block diagram of the experimental set-up for the AOPR TWDM PON system.

total fiber distance between the OLT and the farthest ONU in the system within a single PON link. This number can be calculated as

$$T\_\text{user}_{\text{PON\_link}} = j = s_{\max} \cdot k_{\max} \tag{13}$$

where k is the maximum number of users that can be supported within the 1 × N optical splitter loss. The maximum allowable optical splitter loss can be calculated as

$$\Sigma\alpha_{\text{split}} = \text{Total}_{\text{LLB}} - (\alpha_f L + \alpha_{\text{con}} + \alpha_{\text{splice}} + M_s + W_P). \tag{14}$$

- *Total Users per TWDM PON System* ($T\_\text{user}_{\text{PON System}}$): In the AOPR TWDM PON system, the maximum number of users per entire TWDM PON link is determined using the total number of split ratios m within the entire TWDM PON system. This ratio related to the total fiber distance between the OLT and the farthest ONU in the system within multiple PON links. This number can be calculated as

$$T_{\text{User}_{\text{PON System}}} = m = n \cdot j \tag{15}$$

where n is the total number of PON links; in this case, the system was assumed to have the same link loss budget for all PON links after subtracting the W_p loss margin.

4. Experimental Arrangement of Flexible Packet Broadcasting and the Multicasting XGM Function

The block diagram experimental setup of the XGM to emulate the proposed AOPR TWDM PON system architecture is shown in Fig. 3. Both SOAs (XGM SOA and post-SOA) used in this set-up are Alphion SAC 20r with a peak gain at 25 dB, average noise value at 6.9 dB and power saturation at +13.3 dBm, representing the inline type (high gain). Using an Agilent 10 G BERT, the quality of the signal, e.g., as determined via BER curves, can be correlated with the SOA received input power and the SOA output power, which affect system performance. Point A determines the transmit data power, which represents the data signal from the OLT to the ONU as a downstream signal. Point B is an output probe power representing a new wavelength as the new carrier for the downstream signal. Point C represents the total input power to the SOA (OLT Tx power + total CW pump probe power). Point D represents the received power of the ONU receiver. This set-up requires one SOA located at Point C and the other SOA located just after the AWG. This design focuses on the maximum number of CW probe signal modules that

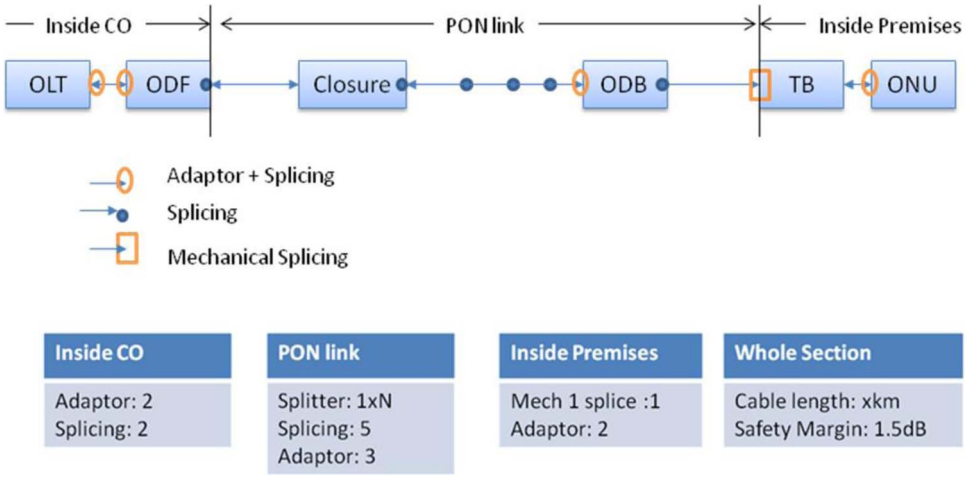

Fig. 4. Typical power attenuation loss in the PON system.

TABLE 1

Type of loss for each component

Type of Loss	Loss (dB)
Fibre Length, $\alpha_f L$	0.25/km
Adaptor, α_{con}	0.2
Fusion Splice, α_{splice}	0.1
Mechanical Splice, α_{splice}	0.3
Safe Margin, S_M	1.5
Wavelength Penalty, W_P	1 (WSS), 2 (All ON)
Splitter Loss, α_{split_loss}	$\alpha_{split} = 3(y) + 0.5$

generate multiple wavelengths to support multicasting and broadcasting signals from the single PON port to multiple PON links. In this study, a 100-GHz channel spacing was used between two adjacent CW PPS modules that used fixed multichannel Agilent DFB laser pumps at a maximum of $+8$ dBm per probe signal. A Finisar transmitter with an output power in the range of -1 to $+3$ dBm, extension ratio of 8.2, side mode suppression ratio (SMSR) of 30 dB and relative intensity noise of -130 dB/Hz was used to emulate the OLT transmitter fixed at 1541.48 nm. For the ONU, a Finisar receiver was used with a received sensitivity of -24 dBm at 9.95 Gb/s with an optical center wavelength at 100 GHz. To route the signal from any PON port to any PON link, the 16 × 16 AWG was used as a passive router with a spacing of 100 GHz, an insertion loss average of 5.5 dB, a ripple of 0.5 dB, a polarization dependence loss (PDL) of 0.4 dB, a chromatic dispersion (CD) of ± 10 ps/nm, and a polarization mode dispersion (PMD) of 0.5 ps. The CW PPS is used as a seeding source to modulate the OLT data onto the new CW; the signal is transmitted at a different power at the wavelength of 1545.47 nm using an Agilent multichannel distributed feedback (DFB) laser source. In this design, the first SOA is designed to support wavelength conversion, and the second SOA (post-amplifier) is introduced to support signal amplification to increase the power margin between the OLT and the ONU. The number of CW PPS signals depends on the mode of operation used in the AOPR TWDM PON system to transmit the CW PPS signals: flexible multicast (multiple signal CW laser will be ON) or All ON.

The maximum allowable link loss margin can be used to determine the maximum distance and the total number of users supported by the system via formulas 9 to 15. The measurement with the consideration of the total attenuation loss is measured as shown in Fig. 4, with each of component loss, as per Table 1. All of the measurements consider realistic numbers for the losses of the connector, splicing, and other components in the system.

5. Result and Discussion of Flexible Packet Broadcasting and Multicasting XGM Function for High Performance of Multichannel Packet Broadcasting and Multicasting Downstream Signal at 10 Gb/s 16-Channel Multicast/Broadcast Wavelengths

To study the performance of the multicasting AOPR TWDM PON system in more detail, the performance of the total transmit power of multiple CW probe channels, as well as the total transmit power of multiple CW PPS signals and the OLT transmit power (CW PPS + OLT Tx) into the SOA for multicasting XGM purposes, were investigated. This study makes a detailed comparison of the correlation between the input powers of both total power signals affecting the XGM performance to generate better BER results. A higher number of CW PPS signals multiplexed into a single fiber increased the total power of the transmitting signal into the SOA and simultaneously decreased the peak power and OSNR of each channel of the CW PPS module. The correlation between the input power, the OLT transmit power, and the CW PPS module significantly affects the BER performance. To maintain the CW PPS input power, a variable or fixed attenuator is used to maintain the performance of the system and reduce the XGM patterning effect.

To support a higher number of PON links connected to a single TWDM PON system, this study analyzed 16 channels of a CW PPS module to support 16 wavelengths with 100 GHz spacing between each channel. Each CW PPS transmitted +8 dBm equally, and all the channels were multiplexed using an AWG as a wavelength multiplexer. Fig. 5 shows the detailed result captured using the OSA. The figures summarize five stages of the signal. The first stage is the combination of the signal from the downstream OLT with 16 channels of the CW PPS module, the second stage is the combination of all of the signals after entering the XGM SOA module, the third stage is after all of the signals were filtered and routed by the AWG prior to being transmitted into their dedicated PON links, the fourth stage is after re-amplification by the post-amplifier and the fifth stage is the signal after reaching the ONU receiver. Fig. 5(a) shows the multiplexing of 16 channels of the CW PPS module with each CW PPS transmit signal at −9.64 dBm. Due to the multiplexing effect, the OSNR value of each CW PPS was reduced to 50.19 dB. Fig. 5(b) shows the combination of the OLT downstream and the 16 channels of the CW PPS module. Each CW PPS transmit signal power is reduced by 2.9 dB to become 512.57 dBm. This reduction affects the OSNR value of the CW PPS module by 48.23 dB. Fig. 5(c) shows the signal after entering the first SOA and experiencing the XGM effect. The power of each CW PPS transmit signal is amplified by nearly 11 dBm to boost the transmit signal to −1.45 dBm. This amplification activity also increased the noise floor level due to ASE generated by the SOA and reduced the OSNR value to 39.55 dB. Fig. 5(d) shows the CW PPS and OLT transmit signal filtered by the AWG. Due to the AWG loss, a selected CW PPS signal is transmitted at −7.36 dBm. This process filtered not only the unwanted signals but also the ASE noise out of the signal band and reduced the OOB OSNR value to 59.64 dBm. The true OSNR is the In Band OSNR value (33.64 dB), which was between the previous ASE noise level created by the first SOA and the peak power of the amplified CW PPS signal. Fig. 5(e) shows the selected CW PPS signal amplified by the second SOA; the signal power is amplified to +9.11 dBm, and the noise floor power level at −35 dBm, resulting in an OSNR value of 44.11 dB. Fig. 5(f) indicates that the signal reaches the ONU receiver at −22.36 dBm with BER of 10^{-4}. The total link loss margin of 31.47 dB was measured between the output post amplifier signal and the ONU received signal.

6. System Design Optimization of the Multiple-Wavelength XGM

The OSNR value at different channels of the CW PPS in each point of transmission is described in Table 2. Using a single-wavelength CW PPS to support the flexible packet routing function, the system enables the OSNR transit signal of the CW PPS module to have an OSNR of 63 dB. After the signal enters the first SOA to support XGM, the OSNR value is found to degrade to 54 dB. Next, although the AWG filters the ASE noise, the in-band OSNR is reduced to 44.59 dB. Using a post-amplifier, the OSNR of the signal improves to 49.25 dB. This trend also applies for

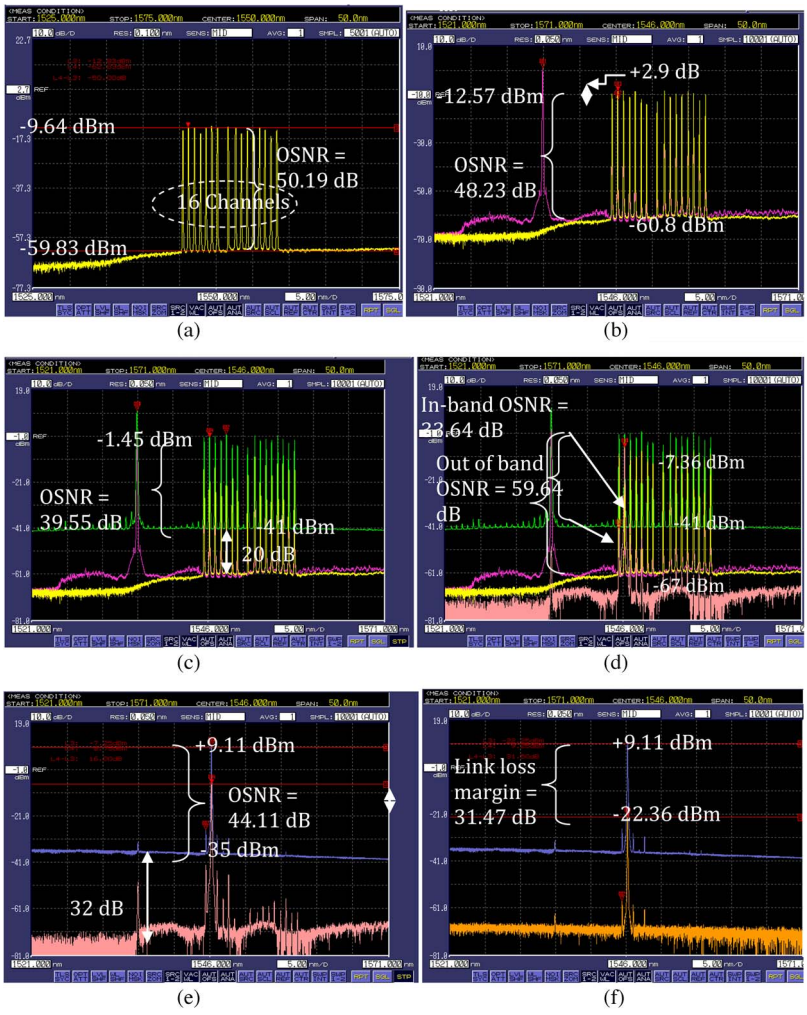

Fig. 5. Result captured using an optical spectrum analyzer. (a) Total of 16 CW probe signals and the OLT downstream signal; (b) signal after the XGM effect that generates an additional ghost signal; (c) total of 16 probe signals after the XGM effect; (d) comparison before and after all 16 probe signals entered the SOA; (e) signal filtered by the AWG; and (f) comparison of the signal before entering the SOA, after entering the SOA and after being filtered by the AWG.

TABLE 2

OSNR value at different numbers of CW PPS signals at different points of the transmission signal

Spectrum point		Single λ CW PPS	4λ CW PPS	16λ CW PPS
CW PPS (after multiplexing)	OSNR (dB)	63	56.68	50.19
After XGM		54	43.98	39.55
After AWG		44.59	37.75	33.64
After post-amplifier		49.25	49.46	44.11
AOPR OLT o/p power (dBm)		+11.25	+11.56	+9.11
AOPR ONU Rx power (dBm)		−23.04	−20.29	−22.36
Loss (dB)		34	31.85	31.47
BER		BER e-8	BER e-8	BER e-3

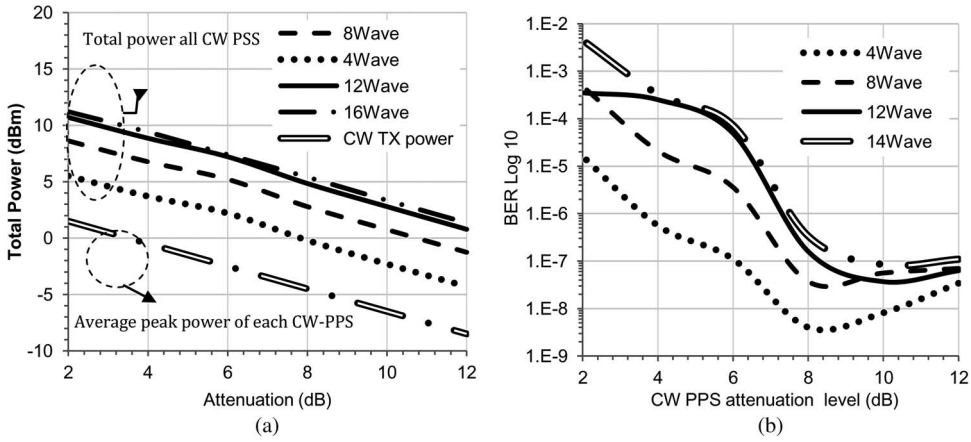

Fig. 6. (a) Different attenuation levels versus the total power of the CW PPS at different CW PPS transmit wavelengths and (b) different attenuation levels versus the BER performance of the system at different CW PPS transmit wavelengths.

the flexible multicasting and broadcasting function. Using four and 16 channels of the CW PPS module, the OSNR value of each CW PPS channel is reduced from 63 dB (single channel) to 56.68 and 50.19 dB, respectively. Because the absolute power of the probe signal is held constant at +8 dBm, increasing the number of CW PPS channels aggregated onto the multiplexer in turn was found to reduce the power of the individual wavelengths. A higher number of CW PPS signals lowers the OSNR value of each CW transmit signal, thereby affecting the overall OSNR at every point of the transmission signal. The table also indicates that the post-amplifier improved the OSNR value, thus improving the performance of the system. The FWM effect is another factor of signal degradation that interferes with the original wavelength in the probe signal if it falls on the same wavelength and induces intraband cross-talk that cannot be filtered out.

As reported in the previous section, the correlation between the input power, the OLT transmit power, and the CW PPS signal significantly affects the BER performance of the system. A variable or fixed attenuator is used to maintain the CW PPS input power, thereby maintaining the performance of the system. Fig. 6(a) shows the total power of the CW PPS module at different numbers of multiplexed wavelengths as well as the average peak power of each CW PPS signal versus the total attenuation value in the system. An optical power meter was used to measure the total received power, and an OSA was used to measure each peak power of the CW PPS module. The total power of the CW PPS module reduced steadily with increasing attenuation power and thus reduced each CW PPS power. However, the OSNR value of each CW PPS remained constant because both the noise floor and the peak power levels were reduced at the same power margin. Fig. 6(b) shows the correlation between the BER performance of the system with the attenuation of the total number of CW PPS signals. In this setup, multiple CW PPS signals were transmitted, and then the total CW PPS power was attenuated before the signals were combined with the OLT transmit signals to enter the XGM SOA. This result indicates that increasing the amount of attenuation of the total power of the CW PPS module improves BER performance within the system. However, this result is applicable until a certain transmitting power (before the BER performances start to saturate and then degrade). This trend indicates that by reducing the total power of the CW PPS module, the total input power into the SOA is reduced and that a certain input power at different gain levels in the output of the SOA signal will impact the OSNR value of the output inverted modulated CW PPS module. The graph shows that the total power of the CW PPS module at four wavelengths requires up to 8 dB attenuation, which is equivalent to 0 dBm CW PPS transmit power. For the CW PPS module operating at 8 wavelengths, the attenuation power level also reaches 8 dB, which is equivalent to +3 dBm CW PPS transmit power. For the CW PPS module operating at 12 and 14 wavelengths, the BER performances generate nearly identical BER lines at a BER of 10^{-7}, which is equivalent to +3 and +4 dBm, respectively, of the total power of the

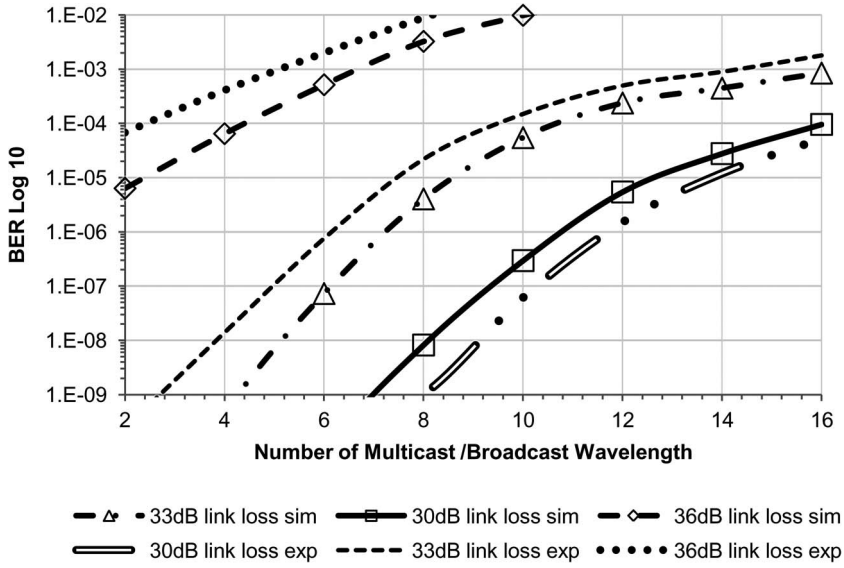

Fig. 7. BER performance of the proposed system with different link loss margins at 10 Gb/s to support up to 16 multicast signal wavelengths.

CW PPS module. However, to achieve the best BER performance, the total power of the CW PPS module must be reduced to 9 dB. In summary, to support the multicasting channel from multiple CW PPS signals, the system can use a fixed-type attenuator because different attenuation power values for a CW PPS module operating at between four and 14 wavelengths are only 1–2 dB. This characteristic reduces the cost of the system. However, to achieve the best performance, implementing a tunable attenuator is the best option to enable the system to support multiple CW PPS signals and generate multicasting signals.

Fig. 7 shows the BER performance of both the simulation and the experimental set-up of a number of multicast wavelengths compared with different numbers of link loss margins between the OLT and the ONU at 10 Gb/s per channel. The graph shows that for a 30-dB link loss margin, the system can support a maximum of up to 16 B&M wavelengths with a minimum BER of 10^{-5} for the simulation and the experimental results. For 33-dB link loss, the system can support 16 B&M wavelengths with a minimum BER of 10^{-3} in the simulation design; however, only 14 broadcast wavelengths can be supported with a minimum BER 8 of 10^{-4} in the experimental design. For a link loss of 36 dB, the system can support up to 6 B&M wavelengths in the simulation design or 5 B&M wavelengths with a minimum BER of 10^{-3}. The difference between the simulation and the experimental design is due to the additional loss or noise in the SOA and the AWG not being considered in the simulation set-up.

In summary, Fig. 8 shows the total number of users at different distance coverages with different numbers of PON links connected to a single TWDM PON system according to a performance below a BER of 10^{-3}. On the basis of equations 9 to 17, the value of W_P is set to 2 dB to support the All ON method. Fig. 8(a) shows the maximum number of users connected to a single PON link at different numbers of multicast wavelengths for different distances. The bar graph shows that the maximum number of users that can be connected to a single PON link is 256 with 4 multicasting wavelengths at a distance of 20 km. However, to support a long-reach PON system of up to 60 km, the system can only handle 16 users per PON link with four multicasting wavelengths. Fig. 8(b) shows the total maximum number of users connected to all PON links in a single AOPR TWDM PON system. The graph shows that the maximum number of users that can be supported is up to 1024, 256 and 64 using four and eight PON links at 20, 40, and 60 km, respectively. The graph also shows that 16 is the maximum number of multicast or PON links that can be handled (with 2048, 512, and 128 users at 20, 40, and 60 km, respectively).

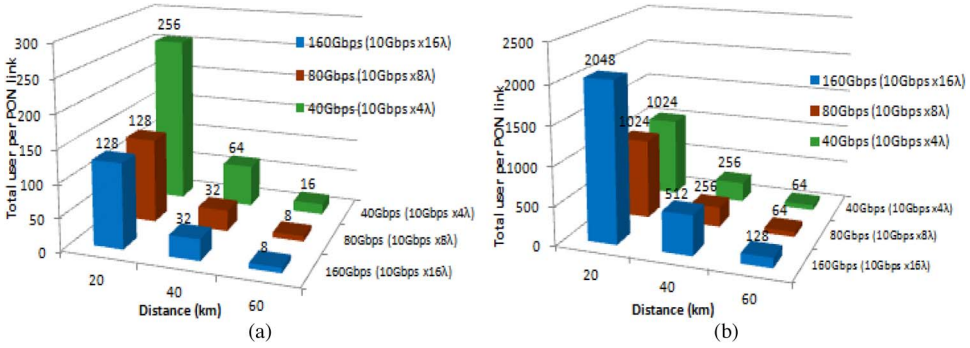

Fig. 8. Summary of the total number of users at different distances and different number of wavelengths at (a) total user per PON link and (b) total user per AOPR TWDM PON system using the All ON method.

7. Conclusion

This paper presented a study of the flexible design of the TWDM PON system architecture, which included the basic structure, principle, implementation, and demonstration. This study showed that the AOPR TWDM PON system as implemented with NG-PON2 can be used to support an extended design of the TWDM PON system. In addition, the system supports the coexistence of the current legacy GPON and XG-PON systems in the proposed architecture. The proposed AOPR TWDM PON system architecture was subjected to both simulation and experimental environments. The AOPR module was designed to incorporate the fixed-type wavelength OLT transmitter with the CW PPS module. This design enables the broadcasting of all OLT downstream signals from any PON port to all PON links, thereby eliminating the packet tuning delays between the PON links. This method would also minimize the laser inventory issue caused by the requirement of different OLT PON port transmitter wavelengths. The OSNR value at different numbers of channels of the CW-PPS module for each transmission point was examined during the development and experimental stages. In accordance to the objective of this study, the result also demonstrated that the proposed system could handle four, eight, and up to 16 PON links with a maximum of 1024, 1204 and 2048 users, respectively. The total loss margin result also demonstrated that the system could cover a long-reach TWDM PON system of up to 60 km with a maximum of 128 and 64 users using 16 PON links and eight PON links, respectively. In conclusion, this work utilized simulations and practical arrangements to produce a new AOPR TWDM PON system architecture by integrating the AOPR and broadcasting or multicasting function based on XGM. The proposed design has the potential to be integrated with the OLT transceiver module and fabricated into the photonic integrated circuit (PIC) form factor to reduce size and minimize power consumption. The system has potential to be implemented in the access network for the future extension of the TWDM PON system.

References

[1] D. Shea and J. Mitchell, "Architecture to integrate multiple PONs with long reach DWDM backhaul," *IEEE J. Sel. Areas Commun.*, vol. 27, no. 2, pp. 126–133, Feb. 2009.
[2] G. Talli and P. Townsend, "Hybrid DWDM-TDM long-reach PON for next-generation optical access," *J. Lightw. Technol.*, vol. 24, no. 7, pp. 2827–2834, Jul. 2006.
[3] K. Taguchi, M. Imai, and T. Suzuki, "Applicable area estimation of bidirectional optical amplifiers to 10-Gb/s class long-reach PON systems," in *Proc. 9th COIN*, 2010, pp. 1–3.
[4] H. Feng, C. Chae, and A. Nirmalathas, "Flexible, low-latency peer-to-peer networking over long-reach WDM/TDM PON systems," in *Proc. 16th OECC*, pp. 186–187, 2011.
[5] K. Taguchi, H. Nakamura, K. Asaka, S. Kimura, and N. Yoshimoto, "Long-reach λ-tunable WDM/TDM-PON using synchronized gain-clamping SOA technology," *J. Opt. Commun. Netw.*, vol. 5, no. 10, pp. 144–151, 2013.
[6] N. Cheng, J. Gao, C. Xu, B. Gao, and D. Liu, "Flexible TWDM PON system with pluggable optical transceiver modules," *Opt. Express*, vol. 22, no. 2, pp. 2078–2090, 2014.

[7] *40-Gigabit-Capable Passive Optical Network (NGPON2): Physical Media Dependent (PMD) Layer Specification*, ITU-T G.989.2, Dec. 2014.
[8] C. Bock, J. Prat, and S. D. Walker, "Hybrid WDM/TDM PON using the AWG FSR and featuring centralized light generation and dynamic bandwidth allocation," *J. Lightw. Technol.*, vol. 23, no. 12, pp. 3981–3988, Dec. 2005.
[9] H. Nakamura *et al.*, "40 Gbit/s-class-wavelength-tunable WDM/TDM-PON using selectable B-Tx and 4 × M cyclic AWG router for flexible photonic aggregation networks," *Opt. Express*, vol. 21, no. 1, pp. 463–468, 2013.
[10] J. Buus and E. J. Murphy, "Tunable lasers in optical networks," *J. Lightw. Technol.*, vol. 24, no. 1, pp. 5–11, Jan. 2006.
[11] J. Fabrega, B. Schrenk, and F. Bo, "Modulated grating Y-structure tunable laser for-routed networks and optical access," *IEEE J. Sel. Top. Quantum Electron.*, vol. 17, no. 6, pp. 1542–1551, Nov./Dec. 2011.
[12] A. Dixit, B. Lannoo, D. Colle, M. Pickavet, and P. Demeester, "Wavelength switched hybrid TDMA/WDM (TWDM) PON: A flexible next-generation optical access solution," in *Proc. 14th Int. Conf. Transparent Opt. Netw.*, Jul. 2012, pp. 1–5.
[13] K. Hara, H. Nakamura, S. Kimura, M. Yoshino, and S. Nishihara, "Flexible load balancing technique using Dynamic Wavelength Bandwidth Allocation (DWBA)," in *Proc. ECOC*, Torino, Italy, 2010, pp. 3–5.
[14] Y. Hsueh and M. Rogge, "A highly flexible and efficient passive optical network employing dynamic wavelength allocation," *Lightw. Technol. J.*, vol. 23, no. 1, pp. 277–286, Jan. 2005.
[15] J. Kani, "Enabling technologies for future scalable and flexible WDM-PON and WDM/TDM-PON systems," *IEEE J. Sel. Top. Quantum Electron.*, vol. 16, no. 5, pp. 1290–1297, Sep./Oct. 2010.
[16] H. Nakamura, "λ-tunable WDM/TDM-PON using DWBA towards flexible next-generation optical access networks," in *Proc. Progr. Electromagn. Res. Symp.*, 2012, pp. 507–510.
[17] M. de la Corte and J. Elmirghani, "Accurate noise characterization of wavelength converters based on XGM in SOAs," *J. Lightw. Technol.*, vol. 21, no. 1, pp. 182–197, Jan. 2003.
[18] B. H. L. Lee, R. Mohamad, and K. Dimyati, "Performance of all-optical multicasting via dual-stage XGM in SOA for grid networking," *IEEE Photon. Technol. Lett.*, vol. 18, no. 21, pp. 2215–2217, Nov. 2006.
[19] P. G. Agrawal, *Fiber-Optic Communication Systems*. Hoboken, NJ, USA: Wiley, 2002.
[20] K. Obermann and K. Petermann, "Estimation of BER performance and cascadability of wavelength converters based on cross-gain modulation in semiconductor optical amplifiers," *Proc. Inst. Elect. Eng.—Optoelectron.*, vol. 147, no. 2, pp. 133–137, Apr. 2000.
[21] R. Davey, "Long-reach passive optical networks," *J. Lightw. Technol.*, vol. 27, no. 3, pp. 273–291, Feb. 2009.
[22] D. Shea and J. Mitchell, "A 10-Gb/s 1024-way-split 100-km long-reach optical-access network," *J. Lightw. Technol.*, vol. 25, no. 3, pp. 685–693, Mar. 2007.
[23] M. de la Corte and J. Elmirghani, "Noise characterisation of wavelength converters based on XGM in SOAs," in *Proc. IEEE GLOBECOM*, 2001, pp. 1541–1545.